

Theoretical analysis of third-harmonic generation via direct third-order and cascaded second-order processes in CsLiB₆O₁₀ crystals

Min-su Kim and Choon Sup Yoon*

Department of Physics, Korea Advanced Institute of Science and Technology, Taejon 305-701, Korea

(Received 24 September 2001; published 1 March 2002)

Third-harmonic generation using a single medium receives theoretical analysis and the results are applied to CsLiB₆O₁₀ crystals. From the solutions for a full set of coupled-amplitude equations, comprehensive expression of overall-effective third-order nonlinear optical susceptibility is derived, including the contributions of direct third-order and cascaded second-order processes. The overall-effective third-order nonlinear optical susceptibility shows peculiar behaviors, such as oscillatory dependence on propagation distance and dependence on azimuthal and polarization angles with inversion symmetry. The optimum conditions for efficient third-harmonic generation are predicted at the phase-matching angles of second-harmonic generation, sum-frequency generation, and third-harmonic generation.

DOI: 10.1103/PhysRevA.65.033831

PACS number(s): 42.65.Ky, 42.70.Mp, 42.65.An

I. INTRODUCTION

Third-harmonic generation (THG) of high intensity using a single nonlinear optical (NLO) medium, instead of two, has been an appealing approach for obtaining coherent ultraviolet (UV) light sources. THG using a single NLO medium is termed “single-medium THG” throughout this paper. Single-medium THG can be realized via direct third-order and cascaded second-order processes [Fig. 1(a)]. Although this idea has received consideration since the beginning of nonlinear optics [1–4], its wide application has been hindered due to the facts that the magnitude of third-order NLO susceptibility $\chi^{(3)}$ in a material is, in general, much smaller than that of second-order NLO susceptibility $\chi^{(2)}$, and a great proportion of efficient NLO crystals are not transparent in the UV region. Given these hindering factors, THG of high-conversion efficiencies of 20–30% has usually been achieved by two successive second-order NLO processes, that is, second-harmonic generation (SHG) followed by sum-frequency generation (SFG) [Fig. 1(b)] [5–7], and single-medium THG has been rarely utilized apart from spectroscopy [8].

In recent years, borate NLO crystals [9–11] of large size and excellent quality, such as β -BaB₂O₄ (BBO), LiB₃O₅ (LBO), and CsLiB₆O₁₀ (CLBO), have become widely available. These crystals have relatively large second-order NLO susceptibilities, high laser-damage thresholds, and wide transparency ranges in the UV region. Combinations developed recently, using borate crystals and high peak-power lasers, make it possible to generate UV light of significant intensity utilizing single-medium THG [12–15]. Major efforts in this direction have been made using BBO crystals [12–14] and a maximum THG conversion efficiency of 6% was achieved [14]. However, previous reports contained a number of significant errors for overall-effective third-order NLO susceptibilities, and interpretations of the experimental data were misleading [12,13,16–18]. CLBO crystals have been developed recently that possess excellent

NLO properties [11,19–22], such as a relatively large second-order NLO coefficient, wide transparency in the UV region, and a high laser-damage threshold [11,19]. CLBO has a number of advantages over BBO and LBO. It possesses higher laser-damage threshold and wider phase-matching (PM) acceptance bandwidth than BBO [19,22], and can satisfy the PM conditions of fourth and fifth harmonics of a Nd:YAG laser [6,23,24], whereas LBO cannot. In addition, CLBO can be grown to a large size with a high degree of perfection in a short time [11,20].

In this paper, a full set of coupled-amplitude equations governing single-medium THG is formulated and the solution is obtained under the undepleted-pump approximation. A comprehensive definition for overall-effective third-order NLO susceptibility is introduced, which is essential for predicting PM characteristics of single-medium THG. Using the definition, overall-effective third-order NLO susceptibilities are calculated, and the PM characteristics and optimum PM conditions are investigated for all possible PM conditions at 1.064 μ m in CLBO crystals.

II. ANALYTIC SOLUTIONS FOR THIRD-HARMONIC FIELD AMPLITUDE

A. Third-harmonic generation in noncentrosymmetric media

When a direct third-order NLO process, shown in Fig. 2(a), satisfies a PM condition along a direction in a noncen-

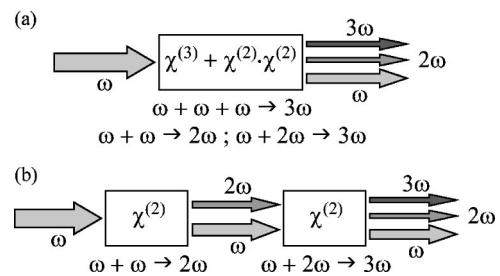


FIG. 1. Schematics of generating third-harmonic waves. (a) Single-medium third-harmonic generation; direct third-order and cascaded second-order processes, and (b) third-harmonic generation using two media; a second-harmonic generation followed by a sum-frequency generation.

*Electronic address: csyoon@mail.kaist.ac.kr

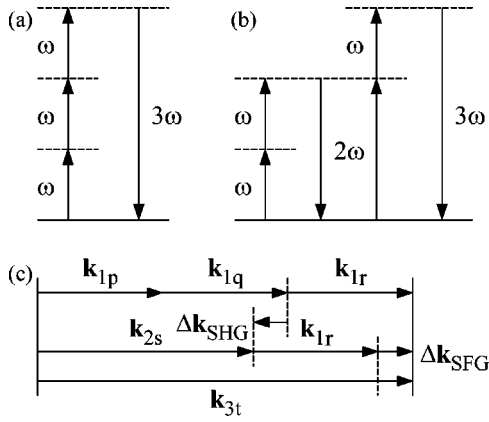


FIG. 2. Energy-level diagrams of third-harmonic generation for (a) direct third-order and (b) cascaded second-order processes. The dashed lines indicate virtual states. (c) Wave-vector diagram of the direct third-order and cascaded second-order processes at the phase-matching condition for the direct third-harmonic generation process. The numbers in subscripts of the wave vectors refer to the order of harmonic waves and the indices p , q , r , s , and t represent polarization states.

triosymmetric medium, the cascaded second-order NLO processes represented by $\chi^{(2)} \cdot \chi^{(2)}$ [Fig. 2(b)] also satisfy the PM condition in the same direction with the same incident wave, although the individual $\chi^{(2)}$ process does not. This is because the amount of wave-vector mismatch Δk_{SHG} occurring in the first second-order process (SHG, $\omega + \omega \rightarrow 2\omega$) is canceled out exactly by the amount of wave-vector mismatch Δk_{SFG} in the subsequent second-order process (SFG, $\omega + 2\omega \rightarrow 3\omega$) [12,25], which is depicted in Fig. 2(c). Therefore, it is expected that not only the direct third-order process, but also the cascaded second-order processes, may equally well contribute to THG as shown in Fig. 1(b) [12]. However, even when the direct third-order NLO process fails to satisfy the PM condition, an efficient THG can still be obtained if the PM condition for either SHG or SFG is met [Fig. 2(b)], since the second-order process that satisfies the PM condition becomes highly effective.

This can be proved by solving coupled-amplitude equations for THG. With the assumption that the incident wave is a collinear, quasicontinuous, and plane wave, a full set of coupled-amplitude equations is given by

$$\begin{aligned} \frac{dA_{1p}}{dz} = & \frac{i\omega}{2n_{1p}c \cos^2 \rho_{1p}} \left[2 \sum_{qs} \chi_{\text{SHG};pqs}^{(2)} A_{1q}^* A_{2s} \right. \\ & \times \exp(-i\Delta k_{pqs}z) + 2 \sum_{st} \chi_{\text{SFG};pst}^{(2)} A_{2s}^* A_{3t} \\ & \times \exp(-i\Delta k_{pst}z) + 3 \sum_{qrt} \chi_{\text{THG};pqrt}^{(3)} A_{1q}^* A_{1r}^* A_{3t} \\ & \left. \times \exp(-i\Delta k_{pqrt}z) \right], \end{aligned} \quad (1)$$

$$\begin{aligned} \frac{dA_{2s}}{dz} = & \frac{2i\omega}{2n_{2s}c \cos^2 \rho_{2s}} \left[\sum_{pq} \chi_{\text{SHG};pqs}^{(2)} A_{1p} A_{1q} \exp(i\Delta k_{pqs}z) \right. \\ & \left. + 2 \sum_{pt} \chi_{\text{SFG};pst}^{(2)} A_{1p}^* A_{3t} \exp(-i\Delta k_{pst}z) \right], \end{aligned} \quad (2)$$

$$\begin{aligned} \frac{dA_{3t}}{dz} = & \frac{3i\omega}{2n_{3t}c \cos^2 \rho_{3t}} \left[2 \sum_{ps} \chi_{\text{SFG};pst}^{(2)} A_{1p} A_{2s} \exp(i\Delta k_{pst}z) \right. \\ & \left. + \sum_{pqr} \chi_{\text{THG};pqrt}^{(3)} A_{1p} A_{1q} A_{1r} \exp(i\Delta k_{pqrt}z) \right]. \end{aligned} \quad (3)$$

Here ρ represents walk-off angle and Δk denotes wave-vector mismatch for a given coupling configuration. $\chi_{\text{SHG};pqs}^{(2)}$ and $\chi_{\text{SFG};pst}^{(2)}$ denote effective second-order NLO susceptibilities for SHG and SFG processes, respectively, and $\chi_{\text{THG};pqrt}^{(3)}$ denotes effective third-order NLO susceptibility for THG process. Subscripts p , q , and r refer to polarization state (e.g., ordinary and extraordinary polarizations in uniaxial crystals) of the fundamental waves, and subscripts s and t indicate the polarization states of second- and third-harmonic waves, respectively. Since the subscripts p , q , r , s , and t in Eqs. (1)–(3) have two polarization states, the full set of equations consists of a total of six equations with a total of 58 coupling terms. Therefore, it is almost impossible to obtain solutions for the above equations analytically. However, the number of coupling terms may be greatly reduced by adopting a proper approximation, and by using symmetry properties of a NLO medium.

When conversion efficiency is sufficiently low, the undepleted-pump approximation can be employed. If we approximate, using the assumption that

$$|A_3| \ll |A_2| \ll |A_1|, \quad (4)$$

Eq. (1), the differential equation for the fundamental wave, can be omitted from the set of coupled-amplitude equations, since dA_{1p}/dz becomes negligible. In addition, Eq. (2) for the second-harmonic wave is reduced to

$$\frac{dA_{2s}}{dz} = \frac{i\omega}{n_{2s}c \cos^2 \rho_{2s}} \sum_{pq} \chi_{\text{SHG};pqs}^{(2)} A_{1p} A_{1q} \exp(i\Delta k_{pqs}z). \quad (5)$$

We can easily obtain the amplitude of the second-order electric field by integrating Eq. (5), and the solution is given by

$$\begin{aligned} A_{2s}(z) = & \sum_{pq} \frac{i\omega \chi_{\text{SHG};pqs}^{(2)} A_{1p} A_{1q}}{n_{2s}c \cos^2 \rho_{2s}} z \\ & \times \exp(i\Delta k_{pqs}z/2) \text{sinc}(\Delta k_{pqs}z/2). \end{aligned} \quad (6)$$

TABLE I. Overall-effective third-order nonlinear optical susceptibilities for single-medium third-harmonic generation in negative uniaxial crystals.

PM condition		$\chi_{\text{eff}}^{(3)}$
SHG	Type I	$\frac{2\chi_{\text{SHG:ooe}}^{(2)}\cos^2\alpha}{3}\left\{\left[\frac{\chi_{\text{SFG:oeo}}^{(2)}\exp(i\Delta k_{\text{SFG:oeo}}z)}{n_{3o}\Delta n_{\text{SFG:oeo}}}+\frac{\chi_{\text{SFG:oee}}^{(2)}\exp(i\Delta k_{\text{SFG:oee}}z)}{n_{3\theta}\Delta n_{\text{SFG:oee}}\cos^2\rho_3}\right]\cos\alpha\right.$ $\left.+\left[\frac{\chi_{\text{SFG:eeo}}^{(2)}\exp(i\Delta k_{\text{SFG:eeo}}z)}{n_{3o}\Delta n_{\text{SFG:eeo}}}+\frac{\chi_{\text{SFG:eee}}^{(2)}\exp(i\Delta k_{\text{SFG:eee}}z)}{n_{3\theta}\Delta n_{\text{SFG:eee}}\cos^2\rho_3}\right]\sin\alpha\right\}$
	Type II	$\frac{2\chi_{\text{SHG:oee}}^{(2)}\sin 2\alpha}{3}\left\{\left[\frac{\chi_{\text{SFG:oeo}}^{(2)}\exp(i\Delta k_{\text{SFG:oeo}}z)}{n_{3o}\Delta n_{\text{SFG:oeo}}}+\frac{\chi_{\text{SFG:oee}}^{(2)}\exp(i\Delta k_{\text{SFG:oee}}z)}{n_{3\theta}\Delta n_{\text{SFG:oee}}\cos^2\rho_3}\right]\cos\alpha\right.$ $\left.+\left[\frac{\chi_{\text{SFG:eeo}}^{(2)}\exp(i\Delta k_{\text{SFG:eeo}}z)}{n_{3o}\Delta n_{\text{SFG:eeo}}}+\frac{\chi_{\text{SFG:eee}}^{(2)}\exp(i\Delta k_{\text{SFG:eee}}z)}{n_{3\theta}\Delta n_{\text{SFG:eee}}\cos^2\rho_3}\right]\sin\alpha\right\}$
SFG	Type I	$-\frac{\chi_{\text{SFG:oee}}^{(2)}\cos\alpha}{n_{2o}}\left[\frac{\chi_{\text{SHG:ooo}}^{(2)}\cos^2\alpha}{\Delta n_{\text{SHG:ooo}}}+\frac{\chi_{\text{SHG:oeo}}^{(2)}\sin 2\alpha}{\Delta n_{\text{SHG:oeo}}}+\frac{\chi_{\text{SHG:eeo}}^{(2)}\sin^2\alpha}{\Delta n_{\text{SHG:eeo}}}\right]$
	Type II	$-\frac{\chi_{\text{SFG:oeo}}^{(2)}\sin\alpha}{n_{2o}}\left[\frac{\chi_{\text{SHG:ooo}}^{(2)}\cos^2\alpha}{\Delta n_{\text{SHG:ooo}}}+\frac{\chi_{\text{SHG:oeo}}^{(2)}\sin 2\alpha}{\Delta n_{\text{SHG:oeo}}}+\frac{\chi_{\text{SHG:eeo}}^{(2)}\sin^2\alpha}{\Delta n_{\text{SHG:eeo}}}\right]$
	Type III	$-\frac{\chi_{\text{SFG:oee}}^{(2)}\cos\alpha}{n_{2\theta}\cos^2\rho_2}\left[\frac{\chi_{\text{SHG:ooe}}^{(2)}\cos^2\alpha}{\Delta n_{\text{SHG:ooe}}}+\frac{\chi_{\text{SHG:oeo}}^{(2)}\sin 2\alpha}{\Delta n_{\text{SHG:oeo}}}+\frac{\chi_{\text{SHG:eee}}^{(2)}\sin^2\alpha}{\Delta n_{\text{SHG:eee}}}\right]$
THG	Type I	$\left[\chi_{\text{THG:oooe}}^{(3)}+\frac{\chi_{\text{SFG:oeo}}^{(2)}\chi_{\text{SHG:ooo}}^{(2)}}{n_{2o}\Delta n_{\text{SHG:ooo}}}+\frac{\chi_{\text{SFG:oee}}^{(2)}\chi_{\text{SHG:oeo}}^{(2)}}{n_{2\theta}\Delta n_{\text{SHG:oeo}}\cos^2\rho_2}\right]\cos^3\alpha$
	Type II	$\left[3\chi_{\text{THG:ooee}}^{(3)}+\frac{\chi_{\text{SFG:oeo}}^{(2)}\chi_{\text{SHG:ooo}}^{(2)}}{n_{2o}\Delta n_{\text{SHG:ooo}}}+\frac{\chi_{\text{SFG:eee}}^{(2)}\chi_{\text{SHG:oeo}}^{(2)}}{n_{2\theta}\Delta n_{\text{SHG:oeo}}\cos^2\rho_2}\right.$ $\left.+\frac{2\chi_{\text{SFG:oeo}}^{(2)}\chi_{\text{SHG:oeo}}^{(2)}}{n_{2o}\Delta n_{\text{SHG:oeo}}}+\frac{2\chi_{\text{SFG:oee}}^{(2)}\chi_{\text{SHG:oee}}^{(2)}}{n_{2\theta}\Delta n_{\text{SHG:oee}}\cos^2\rho_2}\right]\cos^2\alpha\sin\alpha$
	Type III	$\left[3\chi_{\text{THG:oeee}}^{(3)}+\frac{2\chi_{\text{SFG:oeo}}^{(2)}\chi_{\text{SHG:oeo}}^{(2)}}{n_{2o}\Delta n_{\text{SHG:oeo}}}+\frac{2\chi_{\text{SFG:eee}}^{(2)}\chi_{\text{SHG:oee}}^{(2)}}{n_{2\theta}\Delta n_{\text{SHG:oee}}\cos^2\rho_2}\right.$ $\left.+\frac{\chi_{\text{SFG:oeo}}^{(2)}\chi_{\text{SHG:eeo}}^{(2)}}{n_{2o}\Delta n_{\text{SHG:eeo}}}+\frac{\chi_{\text{SFG:oee}}^{(2)}\chi_{\text{SHG:eee}}^{(2)}}{n_{2\theta}\Delta n_{\text{SHG:eee}}\cos^2\rho_2}\right]\cos\alpha\sin^2\alpha$

The amplitude of the third-order electric field also can be obtained by integrating Eq. (3), with Eq. (6) being substituted into Eq. (3). The third-order solution can be expressed as

$$A_{3t}(z) = A_{3t}^{\text{dir}}(z) + A_{3t}^{\text{cas}}(z), \quad (7)$$

where $A_{3t}^{\text{dir}}(z)$ and $A_{3t}^{\text{cas}}(z)$ are given by

$$A_{3t}^{\text{dir}}(z) = \sum_{pqr} \frac{3i\omega\chi_{\text{THG:pqrt}}^{(3)}A_{1p}A_{1q}A_{1r}}{2n_{3t}c\cos^2\rho_{3t}}z$$

$$\times \exp(i\Delta k_{pqrt}z/2)\text{sinc}(\Delta k_{pqrt}z/2), \quad (8)$$

$$A_{3t}^{\text{cas}}(z) = \sum_{pqrs} \frac{3i\omega^2\chi_{\text{SFG:rst}}^{(2)}\chi_{\text{SHG:pqs}}^{(2)}A_{1p}A_{1q}A_{1r}}{n_{2s}n_{3t}c^2\cos^2\rho_{2s}\cos^2\rho_{3t}}$$

$$\times \frac{1}{\Delta k_{pqs}} \left\{ \frac{\exp[i(\Delta k_{pqs} + \Delta k_{rst})z] - 1}{i(\Delta k_{pqs} + \Delta k_{rst})} \right.$$

$$\left. - \frac{\exp(i\Delta k_{rst}z) - 1}{i\Delta k_{rst}} \right\}, \quad (9)$$

and Eqs. (8) and (9) represent the contributions of direct third-order and cascaded second-order processes, respectively. Although Qiu and Penzkofer [12] also derived results similar to Eqs. (8) and (9), they neglected summations over different polarization states of the fundamental and second-

TABLE II. Effective second- and third-order nonlinear optical susceptibilities of CsLiB₆O₁₀.

NLO process	χ_{eff}
SHG ($\omega + \omega \rightarrow 2\omega$)	
$o_1 o_1 \rightarrow o_2$	$\chi_{\text{SHG:ooo}}^{(2)} = 0$
$o_1 o_1 \rightarrow e_2$	$\chi_{\text{SHG:ooe}}^{(2)} = -\chi_{312}^{(2)} \sin(\theta + \rho_2) \sin 2\phi$
$o_1 e_1 \rightarrow o_2$	$\chi_{\text{SHG:oeo}}^{(2)} = -\chi_{123}^{(2)} \sin(\theta + \rho_1) \sin 2\phi$
$o_1 e_1 \rightarrow e_2$	$\chi_{\text{SHG:oee}}^{(2)} = [\chi_{123}^{(2)} \sin(\theta + \rho_1) \cos(\theta + \rho_2) + \chi_{312}^{(2)} \cos(\theta + \rho_1) \sin(\theta + \rho_2)] \cos 2\phi$
$e_1 e_1 \rightarrow o_2$	$\chi_{\text{SHG:eeo}}^{(2)} = \chi_{123}^{(2)} \sin(2\theta + 2\rho_1) \cos 2\phi$
$e_1 e_1 \rightarrow e_2$	$\chi_{\text{SHG:eee}}^{(2)} = [2\chi_{123}^{(2)} \sin(\theta + \rho_1) \cos(\theta + \rho_2) + \chi_{312}^{(2)} \cos(\theta + \rho_1) \sin(\theta + \rho_2)] \cos(\theta + \rho_1) \sin 2\phi$
SFG ($\omega + 2\omega \rightarrow 3\omega$)	
$o_1 o_2 \rightarrow o_3$	$\chi_{\text{SFG:ooo}}^{(2)} = 0$
$o_1 o_2 \rightarrow e_3$	$\chi_{\text{SFG:ooe}}^{(2)} = -\chi_{312}^{(2)} \sin(\theta + \rho_3) \sin 2\phi$
$e_1 o_2 \rightarrow o_3$	$\chi_{\text{SFG:eeo}}^{(2)} = -\chi_{132}^{(2)} \sin(\theta + \rho_1) \sin 2\phi$
$e_1 o_2 \rightarrow e_3$	$\chi_{\text{SFG:eee}}^{(2)} = [\chi_{132}^{(2)} \sin(\theta + \rho_1) \cos(\theta + \rho_3) + \chi_{312}^{(2)} \cos(\theta + \rho_1) \sin(\theta + \rho_3)] \cos 2\phi$
$o_1 e_2 \rightarrow o_3$	$\chi_{\text{SFG:oeo}}^{(2)} = -\chi_{123}^{(2)} \sin(\theta + \rho_2) \sin 2\phi$
$o_1 e_2 \rightarrow e_3$	$\chi_{\text{SFG:oee}}^{(2)} = [\chi_{123}^{(2)} \sin(\theta + \rho_2) \cos(\theta + \rho_3) + \chi_{312}^{(2)} \cos(\theta + \rho_2) \sin(\theta + \rho_3)] \cos 2\phi$
$e_1 e_2 \rightarrow o_3$	$\chi_{\text{SFG:eeo}}^{(2)} = [\chi_{123}^{(2)} \cos(\theta + \rho_1) \sin(\theta + \rho_2) + \chi_{132}^{(2)} \sin(\theta + \rho_1) \cos(\theta + \rho_2)] \cos 2\phi$
$e_1 e_2 \rightarrow e_3$	$\chi_{\text{SFG:eee}}^{(2)} = [\chi_{123}^{(2)} \cos(\theta + \rho_1) \sin(\theta + \rho_2) \cos(\theta + \rho_3) + \chi_{132}^{(2)} \sin(\theta + \rho_1) \cos(\theta + \rho_2) \cos(\theta + \rho_3) + \chi_{312}^{(2)} \cos(\theta + \rho_1) \times \cos(\theta + \rho_2) \sin(\theta + \rho_3)] \sin 2\phi$
THG ($\omega + \omega + \omega \rightarrow 3\omega$)	
$o_1 o_1 o_1 \rightarrow e_3$	$\chi_{\text{THG:oooe}}^{(3)} = \frac{1}{4}(\chi_{1111}^{(3)} - 3\chi_{1122}^{(3)}) \cos(\theta + \rho_3) \sin 4\phi$
$o_1 o_1 e_1 \rightarrow e_3$	$\chi_{\text{THG:ooee}}^{(3)} = \frac{1}{2}(\chi_{1111}^{(3)} - 3\chi_{1122}^{(3)}) \cos(\theta + \rho_1) \cos(\theta + \rho_3) \sin^2 2\phi + \chi_{1122}^{(3)} \cos(\theta + \rho_1) \cos(\theta + \rho_3) + \chi_{3311}^{(3)} \sin(\theta + \rho_1) \sin(\theta + \rho_3)$
$o_1 e_1 e_1 \rightarrow e_3$	$\chi_{\text{THG:oeee}}^{(3)} = -\frac{1}{4}(\chi_{1111}^{(3)} - 3\chi_{1122}^{(3)}) \cos^2(\theta + \rho_1) \cos(\theta + \rho_3) \sin 4\phi$

harmonic waves, which causes significant errors in the results for SHG and SFG-PM conditions.

Equations (8) and (9) can be simplified further by considering the fact that the contributions of NLO interactions at large phase-mismatched conditions are negligibly small. For direct third-order processes, only the terms that satisfy the PM conditions dominate the contribution to THG and, therefore, Eq. (8) can be expressed by only one coupling term with multiplication of a degeneracy factor for a set of polarization states satisfying the PM condition.

For cascaded second-order processes, three different cases can be taken into account for PM conditions: those for SHG, SFG, and THG. When the PM condition for THG is almost satisfied ($\Delta k_{pqs} + \Delta k_{rst} = \Delta k_{pqrt} \rightarrow 0$), Eq. (9) is expressed in a simpler form

$$A_{3t}^{\text{cas}}(z) = \sum_{(pqr),s} \frac{3i\omega^2 \chi_{\text{SFG:rst}}^{(2)} \chi_{\text{SHG:pqs}}^{(2)} A_{1p} A_{1q} A_{1r}}{n_{2s} n_{3t} c^2 \cos^2 \rho_{2s} \cos^2 \rho_{3t}} \times \frac{z}{\Delta k_{pqs}} \exp(i\Delta k_{pqr}z/2) \text{sinc}(\Delta k_{pqr}z/2), \quad (10)$$

where the summation is to be performed over the permutations of the indices p , q , and r that satisfy the PM conditions

for THG, and over all possible values of the index s . When the PM condition for SFG is almost satisfied ($\Delta k_{rst} \rightarrow 0$), Eq. (9) is expressed as

$$A_{3t}^{\text{cas}}(z) = - \sum_{pq,(rs)} \frac{3i\omega^2 \chi_{\text{SFG:rst}}^{(2)} \chi_{\text{SHG:pqs}}^{(2)} A_{1p} A_{1q} A_{1r}}{n_{2s} n_{3t} c^2 \cos^2 \rho_{2s} \cos^2 \rho_{3t}} \frac{z}{\Delta k_{pqs}} \times \exp(i\Delta k_{rst}z/2) \text{sinc}(\Delta k_{rst}z/2). \quad (11)$$

When the PM condition for SHG is almost satisfied ($\Delta k_{pqs} \rightarrow 0$), Eq. (9) is expressed as

$$A_{3t}^{\text{cas}}(z) = \sum_{(pqs),r} \frac{3i\omega^2 \chi_{\text{SFG:rst}}^{(2)} \chi_{\text{SHG:pqs}}^{(2)} A_{1p} A_{1q} A_{1r}}{n_{2s} n_{3t} c^2 \cos^2 \rho_{2s} \cos^2 \rho_{3t}} \frac{z}{\Delta k_{rst}} \times \exp[i(\Delta k_{rst} + \Delta k_{pqs}/2)z] \text{sinc}(\Delta k_{pqs}z/2), \quad (12)$$

after a little algebra. Similar but crude results were obtained in a previous work [12], but the expression near the SHG PM was incorrectly derived, leading to the erroneous conclusion that efficient THG cannot be obtained when the SHG-PM condition is met.

B. Phase-matched third-harmonic generation in uniaxial crystals

In Eqs. (10)–(12), the summations over polarization state can be removed by introducing polarization angle α of the fundamental beam. The amplitudes of ordinary and extraordinary components of the fundamental wave are represented as $A_{1o} = A_1 \cos \alpha$ and $A_{1e} = A_1 \sin \alpha$, respectively, in uniaxial crystals.

The total amplitude $A_3(z)$ of the third-order electric field can be represented by a sum of the amplitudes of ordinary and extraordinary electric fields for the direct and cascaded contributions. $A_3(z)$ is expressed, very near the THG and SFG-PM conditions, as

$$A_3(z) = \frac{3i\omega \mathcal{X}_{\text{eff}}^{(3)}(\alpha)}{2n_{3\theta}c \cos^2 \rho_3} A_1^3 z \exp(i\Delta kz/2) \text{sinc}(\Delta kz/2), \quad (13)$$

and very near the SHG-PM conditions, $A_3(z)$ is expressed as

$$A_3(z) = \frac{3i\omega \mathcal{X}_{\text{eff}}^{(3)}(\alpha)}{2n_{2\theta}c \cos^2 \rho_2} A_1^3 z \exp(i\Delta kz/2) \text{sinc}(\Delta kz/2). \quad (14)$$

Here $\mathcal{X}_{\text{eff}}^{(3)}$ denotes overall-effective third-order NLO susceptibility and Δk the wave-vector mismatch for the given PM configuration. In Eqs. (13) and (14), $n_{i\theta}$ ($i=1,2,3$) was used for the refractive index of an extraordinary wave, instead of $n_{ie}(\theta)$, and ρ_i for the walk-off angle of an extraordinary wave, instead of ρ_{ie} , since the walk-off angle ρ_{io} of an ordinary wave is zero.

The expressions for $\mathcal{X}_{\text{eff}}^{(3)}$ very near the PM conditions are listed in Table I for negative uniaxial crystals. The formulas can be readily modified for the cases of positive uniaxial and biaxial systems. The index-mismatch parameters $\Delta n_{\text{SHG}:pqst}$ and $\Delta n_{\text{SFG}:rst}$ are defined as

$$\Delta n_{\text{SHG}:pqst} \equiv \frac{\Delta k_{\text{SHG}:pqst} c}{2\omega} = \frac{n_{1p} + n_{1q}}{2} - n_{2s}, \quad (15)$$

$$\Delta n_{\text{SFG}:rst} \equiv \frac{\Delta k_{\text{SFG}:rst} c}{3\omega} = \frac{n_{1r} + 2n_{2s}}{3} - n_{3t}. \quad (16)$$

It is worth noting that, from Eqs. (13) and (14), TH intensity is proportional to a product of $|\mathcal{X}_{\text{eff}}^{(3)}|^2$ and $\text{sinc}^2(\Delta kz/2)$. Therefore, very near the SFG and THG-PM conditions, the dependence of the TH intensity on the phase mismatch has an envelope of the square of the sinc function, but very near the SHG-PM condition, its shape departs from the envelope of the square of the sinc function, since $|\mathcal{X}_{\text{eff}}^{(3)}|^2$ contains various phase terms very near the SHG-PM condition, as listed in Table I.

III. THIRD-HARMONIC GENERATION IN CsLiB₆O₁₀ CRYSTALS

A. Optical properties of CLBO crystals

CLBO [11,19–22] is a negative uniaxial crystal belonging to the tetragonal $I\bar{4}2d-\bar{4}2m$ class. The transparency of CLBO crystals ranges from 180 to 2750 nm [11]. Although the UV cutoff wavelength of CLBO is slightly longer than that of LBO, the PM property of CLBO for UV generation is much better than LBO owing to large birefringence. CLBO exhibits a very high laser-damage threshold of 26 GW/cm² at 1.064 μm with 1.1-ns pulse duration, which is similar to that of LBO, but much higher than that of BBO [19]. The second-order NLO susceptibility tensor of CLBO has two independent components d_{14} and d_{36} , and the two components are identical under Kleinman's symmetry condition [26]. The reported value of d_{36} is 0.95 pm/V at 1.064 μm [11]. Although the effective second-order NLO coefficient d_{eff} of CLBO is about 60% of that of BBO, CLBO possesses a number of advantages over BBO for high-intensity UV generation, such as higher laser-damage threshold, smaller walk-off angle, and larger angular, spectral, and temperature PM acceptance bandwidths [22]. In addition, CLBO crystals of large size and excellent quality can be grown in a short time [11,20].

The dispersion of the principal refractive indices of CLBO is represented by a set of Sellmeier equations [19],

$$n_o^2 = 2.20490 + \frac{1.10259 \times 10^{-2}}{\lambda^2 - 1.18119 \times 10^{-2}} - 6.95625 \times 10^{-5} \lambda^2, \quad (17a)$$

$$n_e^2 = 2.05936 + \frac{8.64948 \times 10^{-3}}{\lambda^2 - 1.28929 \times 10^{-2}} - 2.67532 \times 10^{-5} \lambda^2, \quad (18a)$$

where λ , the wavelength in μm , lies between 0.240 μm and 0.633 μm , and

$$n_o^2 = 2.14318 + \frac{1.58749 \times 10^{-1}}{\lambda^2 + 1.37559} - 6.23750 \times 10^{-4} \lambda^2, \quad (17b)$$

$$n_e^2 = 2.04195 + \frac{2.73245 \times 10^{-2}}{\lambda^2 + 2.86672 \times 10^{-1}} - 3.42718 \times 10^{-4} \lambda^2, \quad (18b)$$

where λ lies between 0.633 μm and 1.064 μm . Although a number of Sellmeier equations for CLBO crystals have been reported by several authors [11,19,21,22,24], those given by Eqs. (17) and (18) agree best with our measured PM angles [27].

B. Theoretical consideration for single-medium THG in CLBO

The third-order NLO susceptibility tensor $\chi_{ijkl}^{(3)}$ of CLBO has 21 nonzero components, of which only 11 are independent. Since three interacting frequencies are degenerate in

TABLE III. Characteristic parameters for phase-matched single-medium third-harmonic generation at 1.064 μm in $\text{CsLiB}_6\text{O}_{10}$.

PM condition	NLO process	θ_{PM} (deg)	$\Delta\theta L$ (deg mm)	ρ_1 (deg)	ρ_2 (deg)	ρ_3 (deg)	n_2	n_3	Δn	Δk (mm^{-1})
SHG										
Type I	$o_1o_1 \rightarrow e_2$	29.63	0.584	1.70	1.78	1.87	1.4852		0	0
	$o_1e_2 \rightarrow e_3$							1.5029	-0.0177	-314.13
	$e_1e_2 \rightarrow e_3$							1.5029	-0.0219	-388.57
	$o_1e_2 \rightarrow o_3$							1.5171	-0.0319	-565.31
Type II	$e_1e_2 \rightarrow o_3$	43.28	0.980	1.95	2.04	2.14	1.4732		0	0
	$o_1e_1 \rightarrow e_2$							1.4902	-0.0130	-230.04
	$o_1e_2 \rightarrow e_3$							1.4902	-0.0210	-371.48
	$o_1e_2 \rightarrow o_3$							1.5171	-0.0399	-706.75
	$e_1e_2 \rightarrow o_3$						1.5171	-0.0479	-848.18	
SFG										
Type I	$o_1o_2 \rightarrow e_3$	39.27	0.327	1.92	2.01	2.11		1.4941	0	0
	$o_1o_1 \rightarrow o_2$						1.4985	-0.0133	-157.32	
	$o_1e_1 \rightarrow o_2$						1.4985	-0.0236	-278.32	
	$e_1e_1 \rightarrow o_2$						1.4985	-0.0338	-399.33	
Type II	$e_1o_2 \rightarrow e_3$	49.34	0.471	1.91	2.00	2.10	1.4843	0	0	
	$o_1o_1 \rightarrow o_2$						1.4985	-0.0133	-157.32	
	$o_1e_1 \rightarrow o_2$						1.4985	-0.0279	-329.56	
	$e_1e_1 \rightarrow o_2$						1.4985	-0.0425	-501.80	
THG										
Type I	$o_1o_1o_1 \rightarrow e_3$	48.45	0.329	1.92	2.01	2.11		1.4852	0	0
	$\{o_1o_1 \rightarrow e_2;$						1.4685	0.0167	197.05	
	$o_1e_2 \rightarrow e_3\}$						1.4852	-0.0111	-197.05	
	$\{o_1o_1 \rightarrow o_2;$						1.4985	-0.0133	-157.32	
Type II	$o_1o_2 \rightarrow e_3\}$	64.02	0.607	1.50	1.57	1.65		1.4852	0.0089	157.32
	$o_1o_1e_1 \rightarrow e_3$						1.4717	0	0	
	$\{o_1o_1 \rightarrow e_2;$						1.4558	0.0294	347.23	
	$e_1e_2 \rightarrow e_3\}$						1.4717	-0.0196	-347.23	
	$\{o_1e_1 \rightarrow e_2;$						1.4558	0.0092	108.18	
	$o_1e_2 \rightarrow e_3\}$						1.4717	-0.0061	-108.18	
	$\{o_1o_1 \rightarrow o_2;$						1.4985	-0.0133	-157.32	
	$e_1o_2 \rightarrow e_3\}$						1.4717	0.0089	157.32	
$\{o_1e_1 \rightarrow o_2;$	1.4985	-0.0336	-396.36							
	$o_1o_2 \rightarrow e_3\}$						1.4717	0.0224	396.36	

THG processes, only $\chi_{1111}^{(3)}$, $\chi_{1122}^{(3)}$, $\chi_{1133}^{(3)}$, $\chi_{3311}^{(3)}$, and $\chi_{3333}^{(3)}$ remain independent, due to the permutation symmetry of indices j, k , and l . The second-order NLO susceptibility $\chi_{ijk}^{(2)}$ of CLBO has two independent components $\chi_{123}^{(2)}$ ($=2d_{14}$) and $\chi_{312}^{(2)}$ ($=2d_{36}$) for SHG, and three independent components $\chi_{123}^{(2)}$, $\chi_{132}^{(2)}$, and $\chi_{312}^{(2)}$ for SFG. In a uniaxial crystal, the polarization unit vectors for ordinary and extraordinary waves are expressed in polar coordinates as

$$\mathbf{e}_o = (\sin \phi, -\cos \phi, 0), \quad (19)$$

$$\mathbf{e}_e = (-\cos(\theta + \rho)\cos \phi, -\cos(\theta + \rho)\sin \phi, \sin(\theta + \rho)). \quad (20)$$

Using Eqs. (19) and (20), the effective second-order NLO susceptibilities for SHG and SFG, and the effective third-order NLO susceptibility for THG of CLBO are represented in Table II.

The effective second-order NLO susceptibility can be calculated if all the components of the second-order NLO susceptibility tensor are known. Among the values of $\chi_{ijk}^{(2)}$, only $\chi_{312}^{(2)}$ for SHG is reported, which is 1.90 pm/V at 1.064 μm [11]. All the other tensor components, $\chi_{123}^{(2)}$ for SHG, $\chi_{123}^{(2)}$ and $\chi_{132}^{(2)}$ for SFG, are identical to $\chi_{312}^{(2)}$ for SHG and SFG, respectively, if we apply Kleinman's symmetry condition, which is based on the assumption that the dispersion of nonlinearity is negligible. This condition is well satisfied for CLBO, since the UV cutoff wavelength (0.180 μm) of

TABLE IV. Overall-effective third-order nonlinear optical susceptibilities for single-medium third-harmonic generation at 1.064 μm in $\text{CsLiB}_6\text{O}_{10}$.

PM condition		$\mathcal{X}_{\text{eff}}^{(3)} (\text{pm}^2/\text{V}^2)$
SHG	Type I	$-0.6601\{[21.96 \exp(-565.3iz) \sin^2 2\phi - 34.11 \exp(-314.1iz) \sin 4\phi] \cos \alpha$ $- [16.55 \exp(-639.8iz) \sin 4\phi + 70.55 \exp(-388.6iz) \sin^2 2\phi] \sin \alpha\} \cos^2 \alpha$
	Type II	$1.267\{[11.98 \exp(-706.8iz) \sin 4\phi - 105.6 \exp(-230.0iz) \cos^2 2\phi] \cos \alpha$ $- [28.08 \exp(-848.2iz) \cos^2 2\phi + 34.47 \exp(-371.5iz) \sin 4\phi] \sin \alpha\} \sin 2\alpha$
SFG	Type I	$0.4500[106.2 \sin^2 2\phi \cos \alpha - 27.84 \sin 4\phi \sin \alpha] \sin 2\alpha$
	Type II	$-1.328[53.09 \sin 4\phi \cos \alpha - 43.65 \cos^2 2\phi \sin \alpha] \sin^2 \alpha$
THG	Type I	$[0.1588(\chi_{1111}^{(3)} - 3\chi_{1122}^{(3)}) - 59.94] \sin 4\phi \cos^3 \alpha$
	Type II	$\{329.4 + 0.5122\chi_{1122}^{(3)} + 2.488\chi_{3311}^{(3)} - [495.7 - 0.2561(\chi_{1111}^{(3)} - 3\chi_{1122}^{(3)})] \sin^2 2\phi\} \cos^2 \alpha \sin \alpha$

CLBO is much shorter than the fundamental (1.064 μm) and harmonic (0.532 μm and 0.355 μm) wavelengths. In addition, $\chi_{312}^{(2)}$ for SFG can be obtained using Miller's rule [28,29]

$$d_{ijk}(\omega_3; \omega_1, \omega_2) = \delta_{ijk} \chi_{ii}^{(1)}(\omega_3) \chi_{jj}^{(1)}(\omega_1) \chi_{kk}^{(1)}(\omega_2), \quad (21)$$

where the Miller's δ_{ijk} is determined by using $\chi_{312}^{(2)} = 1.90 \text{ pm/V}$ for SHG. $\chi_{312}^{(2)}$ for SFG of 1.064 μm and 0.532 μm is calculated to be 2.04 pm/V . However, it is not possible to calculate the effective third-order NLO susceptibility $\chi_{\text{THG}}^{(3)}$ directly from $\chi_{ijkl}^{(3)}$ because no $\chi_{ijkl}^{(3)}$ values of CLBO are available. Nevertheless, the effective third-order NLO susceptibility can be estimated from a measured overall-effective third-order NLO susceptibility $\mathcal{X}_{\text{eff}}^{(3)}$ and the amount of contributions of cascaded second-order processes, which can be calculated using $\chi_{ijk}^{(2)}$, as reported in previous works [12–18].

For single-medium THG at 1.064 μm in CLBO, there exist six types of possible PM conditions: type-I and type-II SHG, type-I and type-II SFG, and type-I and type-II THG. No PM angle is available for type-III SFG and type-III THG. PM angle, walk-off angle, and other related parameters for each PM condition were calculated using Eqs. (17) and (18), which are listed in Table III, where θ_{PM} and $\Delta\theta L$ represent the PM angle and angular acceptance bandwidth, respectively, with L being the sample length. Using the parameters in Table III, $\mathcal{X}_{\text{eff}}^{(3)}$ for different types of PM conditions are represented for single-medium THG at 1.064 μm , with the unknown $\chi_{ijkl}^{(3)}$ components (Table IV). It should be noted that $\mathcal{X}_{\text{eff}}^{(3)}$ for SHG PM has a dependence on propagation distance z , in millimeter. Since $I_{3\omega} \propto |\mathcal{X}_{\text{eff}}^{(3)}|^2$, the TH intensity depends on polarization angle α and azimuthal angle ϕ . Therefore, we can predict the optimum PM conditions that produce the maximum TH intensity.

IV. NUMERICAL CALCULATIONS OF $\mathcal{X}_{\text{eff}}^{(3)}$ AND DISCUSSIONS

For SHG-PM conditions, the expressions for $\mathcal{X}_{\text{eff}}^{(3)}$ in Table IV are rather complicated, which are functions of propagation distance z . Therefore, it is not easy to determine

the optimum PM conditions for single-medium THG. Figure 3 exhibits the dependence of $|\mathcal{X}_{\text{eff}}^{(3)}|$ on propagation distance at the PM angle $\theta_{\text{PM}} = 29.6^\circ$ of type-I SHG. At $\alpha = 0^\circ$ and $\phi = 45^\circ$, which gives the optimum PM condition for type-I SHG, $|\mathcal{X}_{\text{eff}}^{(3)}|$ has a constant value [solid curve in Fig. 3(a)]. However, $\mathcal{X}_{\text{eff}}^{(3)}$ becomes zero when ϕ is 0° or 90° . In general, $|\mathcal{X}_{\text{eff}}^{(3)}|$ shows an oscillatory behavior. For example, at $\alpha = 0^\circ$ and $\phi = 22.5^\circ$, the interference of two nonzero amplitudes with different phase factors gives rise to a sinusoidal oscillation with a period of about 25 μm [dashed curve in Fig. 3(a)]. Thus even a minute change in sample length or propagation direction can lead to a significant variation of the TH intensity by up to a factor of 4, because of the sensitive dependence of $\mathcal{X}_{\text{eff}}^{(3)}$ on the propagation distance.

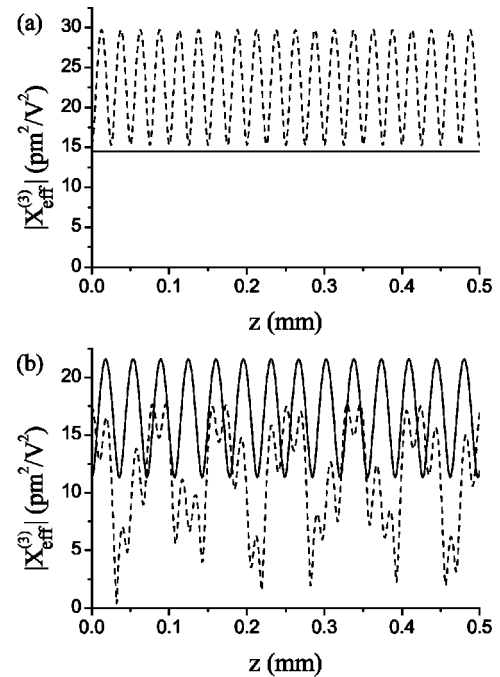


FIG. 3. Dependence of $\mathcal{X}_{\text{eff}}^{(3)}$ on propagation distance at the phase-matching angle of type-I second-harmonic generation with (a) $\alpha = 0^\circ$ and (b) $\alpha = 45^\circ$. The solid curves represent values obtained at $\phi = 45^\circ$ and the dashed curves at $\phi = 22.5^\circ$.

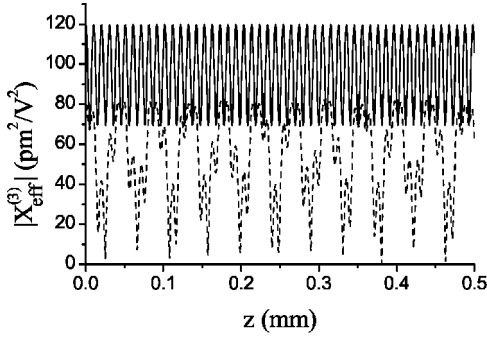


FIG. 4. Dependence of $\chi_{\text{eff}}^{(3)}$ on propagation distance at the phase-matching angle of type-II second-harmonic generation with $\alpha=45^\circ$. The solid curve represents values obtained at $\phi=0^\circ$ and the dashed curve at $\phi=22.5^\circ$.

Nonetheless, the condition of $\alpha=0^\circ$ and $\phi=22.5^\circ$ always produces more efficient single-medium THG than the condition of $\alpha=0^\circ$, $\phi=45^\circ$, due to the larger $|\chi_{\text{eff}}^{(3)}|$ value at $\alpha=0^\circ$, $\phi=22.5^\circ$. Taking another example, the case in which $\alpha=45^\circ$ and $\phi=45^\circ$ yields a sinusoidal oscillation with a period of $35 \mu\text{m}$ [solid curve in Fig. 3(b)]. On the other hand, in the case of $\alpha=45^\circ$, $\phi=22.5^\circ$, the interference of four nonzero amplitudes with different phase factors causes $|\chi_{\text{eff}}^{(3)}|$ to show a complicated oscillatory behavior [dashed curve in Fig. 3(b)]. Figure 4 shows the dependence of $|\chi_{\text{eff}}^{(3)}|$ on propagation distance z at the PM angle $\theta_{\text{PM}}=43.3^\circ$ of type-II SHG with $\alpha=45^\circ$, $\phi=0^\circ$ (solid curve) and $\alpha=45^\circ$, $\phi=22.5^\circ$ (dashed curve). The overall features are very similar to those of Fig. 3(b), but the oscillation periods are much shorter and the maximum values of $|\chi_{\text{eff}}^{(3)}|$ are much larger.

The three-dimensional contour maps of $\chi_{\text{eff}}^{(3)}$ as functions of α and ϕ are shown for the PM conditions of type-I SFG ($\theta_{\text{PM}}=39.3^\circ$) [Fig. 5(a)] and type-II SFG ($\theta_{\text{PM}}=49.3^\circ$) [Fig. 5(b)]. It is noteworthy that the distribution of $\chi_{\text{eff}}^{(3)}$ values is asymmetric with respect to α and ϕ , and the origin in each contour map is, in fact, the inversion center, which is very unlike the features of second-order NLO processes. The optimum PM conditions for single-medium THG can be achieved at $\alpha \approx 36^\circ$, $\phi \approx 50^\circ$ for type-I SFG PM, and at $\alpha=90^\circ$, $\phi=0^\circ$ for type-II SFG PM, and the $\chi_{\text{eff}}^{(3)}$ values reach up to $38 \text{ pm}^2/\text{V}^2$ and $58 \text{ pm}^2/\text{V}^2$, respectively.

In Table IV, it is easy to see that the optimum PM condition for type-I THG ($\theta_{\text{PM}}=48.5^\circ$) of $1.064 \mu\text{m}$ is $\alpha=0^\circ$, $\phi=22.5^\circ$ or 67.5° , regardless of the value of $\chi_{ijkl}^{(3)}$. For type-II THG PM ($\theta_{\text{PM}}=64.0^\circ$), the optimum value of α is also easily determined as 35.3° . However, the optimum value of ϕ depends on the values of $\chi_{ijkl}^{(3)}$ components. The dependence of $\chi_{\text{eff}}^{(3)}$ on ϕ can be expressed in the form of $(A - B \sin^2 \phi)^2$, where the parameters A and B are expressed with linear combinations of $\chi_{ijkl}^{(3)}$. The optimum value of ϕ is 0° for $A/B > 0.5$, and 45° for $A/B < 0.5$. If we consider only cascaded second-order contributions to $\chi_{\text{eff}}^{(3)}$, A/B is calculated to be 0.665 and thus $\chi_{\text{eff}}^{(3)}$ may have the maximum at $\phi=0^\circ$.

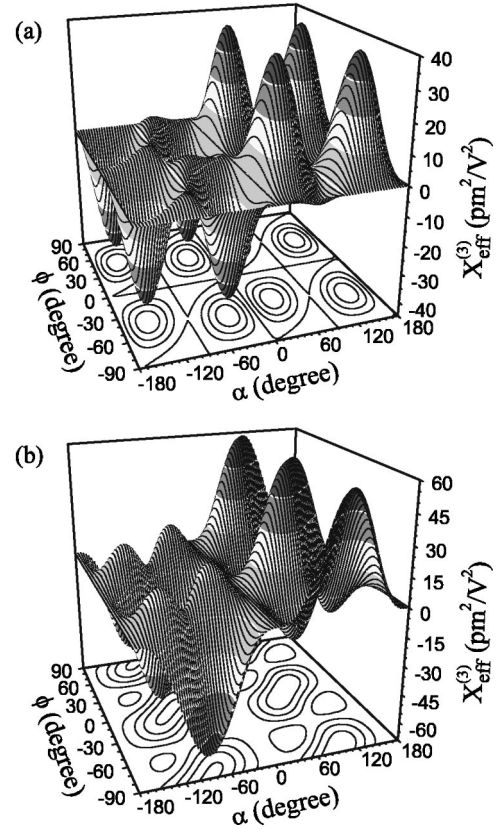


FIG. 5. Three-dimensional contour maps of $\chi_{\text{eff}}^{(3)}$ at the phase-matching angles of sum-frequency generation for (a) type I and (b) type II.

V. CONCLUSIONS

We have investigated theoretically the characteristics of PM and third-order NLO susceptibility for single-medium THG via direct and cascaded processes in CLBO. A full set of coupled-amplitude equations for the general case of single-medium THG were setup and solutions for the TH amplitude was derived. An overall-effective third-order NLO susceptibility $\chi_{\text{eff}}^{(3)}$ was defined, which is essential for predicting the TH intensity. Numerical analysis shows that $\chi_{\text{eff}}^{(3)}$ near SHG-PM conditions is expressed as an oscillatory function of propagation distance. Nevertheless, large $\chi_{\text{eff}}^{(3)}$ values of about 70 to $120 \text{ pm}^2/\text{V}^2$ can be obtained for type-II SHG-PM conditions. For SFG-PM conditions, $\chi_{\text{eff}}^{(3)}$ as a function of α and ϕ shows an inversion symmetry with respect to $\alpha=0^\circ$, $\phi=0^\circ$, and the optimum PM conditions for single-medium THG are $\theta=39.3^\circ$, $\phi \approx 50^\circ$, and $\alpha \approx 36^\circ$ for type-I SFG PM, and $\theta=49.3^\circ$, $\phi=0^\circ$, and $\alpha=90^\circ$ for type-II SFG PM. The optimum PM condition for type-I THG is $\theta=48.5^\circ$, $\phi=22.5^\circ$, and $\alpha=0^\circ$, and that for type-II THG is $\theta=64.0^\circ$, $\alpha=35.3^\circ$, and $\phi=0^\circ$ or 45° , depending on the magnitudes of the third-order NLO susceptibility components $\chi_{ijkl}^{(3)}$.

ACKNOWLEDGMENTS

This work was supported in part by the HAN project and in part by the basic research fund of KAIST.

- [1] J. A. Armstrong, N. Bloembergen, J. Ducuing, and P. S. Pershan, *Phys. Rev.* **127**, 1918 (1962).
- [2] R. W. Terhune, P. D. Maker, and C. M. Savage, *Appl. Phys. Lett.* **2**, 54 (1963).
- [3] P. D. Maker and R. W. Terhune, *Phys. Rev.* **137**, A801 (1965).
- [4] C. C. Wang and E. L. Baardsen, *Appl. Phys. Lett.* **15**, 396 (1969).
- [5] B. Wu, N. Chen, C. Chen, D. Deng, and Z. Xu, *Opt. Lett.* **14**, 1080 (1989).
- [6] T. Zhang, Y. Motoki, L. B. Sharma, H. Daido, Y. Kato, Y. Mori, and T. Sasaki, *Electron. Lett.* **32**, 452 (1996).
- [7] Z. Wang, K. Fu, X. Xu, X. Sun, H. Jiang, R. Song, J. Liu, J. Wang, Y. Liu, J. Wei, and Z. Shao, *Appl. Phys. B: Lasers Opt.* **72**, 839 (2001).
- [8] S. A. Akhmanov and N. I. Koroteev, *Zh. Éksp. Teor. Fiz.* **67**, 1306 (1974) [*Sov. Phys. JETP* **40**, 650 (1975)].
- [9] D. Eimerl, L. Davis, S. Velsko, E. K. Graham, and A. Zalkin, *J. Appl. Phys.* **62**, 1968 (1987).
- [10] D. N. Nikogosyan, *Appl. Phys. A: Solids Surf.* **58**, 181 (1994).
- [11] Y. Mori, I. Kuroda, S. Nakajima, T. Sasaki, and S. Nakai, *Appl. Phys. Lett.* **67**, 1818 (1995).
- [12] P. Qiu and A. Penzkofer, *Appl. Phys. B: Photophys. Laser Chem.* **45**, 225 (1988).
- [13] I. V. Tomov, B. Van Woutherghem, and P.M. Rentzepis, *Appl. Opt.* **31**, 4172 (1992).
- [14] P. S. Banks, M. D. Feit, and M. D. Perry, *Opt. Lett.* **24**, 4 (1999).
- [15] B. Boulanger, J. P. Fève, P. Delarue, I. Rousseau, and G. Marnier, *J. Phys. B* **32**, 475 (1999).
- [16] S. A. Akhmanov, L. B. Meisner, S. T. Parinov, S. M. Saltiel, and V. G. Tunkin, *Zh. Éksp. Teor. Fiz.* **73**, 1710 (1977) [*Sov. Phys. JETP* **46**, 898 (1977)].
- [17] G. R. Meredith, *Phys. Rev. B* **24**, 5522 (1981).
- [18] C. Bosshard, U. Gubler, P. Kaatz, W. Mazerant, and U. Meier, *Phys. Rev. B* **61**, 10 688 (2000).
- [19] Y. Mori, I. Kuroda, S. Nakajima, T. Sasaki, and S. Nakai, *Jpn. J. Appl. Phys., Part 2* **34**, L296 (1995).
- [20] T. Sasaki, Y. Mori, I. Kuroda, S. Nakajima, K. Yamaguchi, and S. Watanabe, *Acta Crystallogr., Sect. C: Cryst. Struct. Commun.* **C51**, 2222 (1995).
- [21] G. Ryu, C. S. Yoon, T. P. J. Han, and H. G. Gallagher, *J. Cryst. Growth* **191**, 492 (1998).
- [22] T. Sasaki, Y. Mori, M. Yoshimura, Y. K. Yap, and T. Kamimura, *Mater. Sci. Eng., R* **30**, 1 (2000).
- [23] Y. K. Yap, M. Inagaki, S. Nakajima, Y. Mori, and T. Sasaki, *Opt. Lett.* **21**, 1348 (1996).
- [24] N. Umemura and K. Kato, *Appl. Opt.* **36**, 6794 (1997).
- [25] S. A. Akhmanov, A. I. Kovrygin, and A. P. Sukhorukov, in *Quantum Electronics: A Treatise*, edited by H. Rabin and C. L. Tang (Academic, New York, 1975), Vol. I, Part B, Chap. 8.
- [26] D. A. Kleinman, *Phys. Rev.* **126**, 1977 (1962).
- [27] M. -s. Kim and C. S. Yoon, in *CLEO/Pacific Rim 2001*, Technical Digest of the 4th Pacific Rim Conference on Lasers and Electro-Optics, Chiba, Japan (IEEE, Piscataway, 2001), Vol. II, p. 398.
- [28] R. C. Miller, *Appl. Phys. Lett.* **5**, 17 (1964).
- [29] C. G. B. Garrett and F. N. H. Robinson, *IEEE J. Quantum Electron.* **2**, 328 (1966).